Light-trapping optimization in wet-etched silicon photonic crystal solar cells

Sergey Eyderman, Sajeev John, M. Hafez, S. S. Al-Ameer, T. S. Al-Harby, Y. Al-Hadeethi, and D. M. Bouwes

Articles you may be interested in

An efficient light trapping scheme based on textured conductive photonic crystal back reflector for performance improvement of amorphous silicon solar cells
Appl. Phys. Lett. **105**, 073506 (2014); 10.1063/1.4893606

Solar light trapping in slanted conical-pore photonic crystals: Beyond statistical ray trapping
J. Appl. Phys. **113**, 154315 (2013); 10.1063/1.4802442

Photonic assisted light trapping integrated in ultrathin crystalline silicon solar cells by nanoimprint lithography
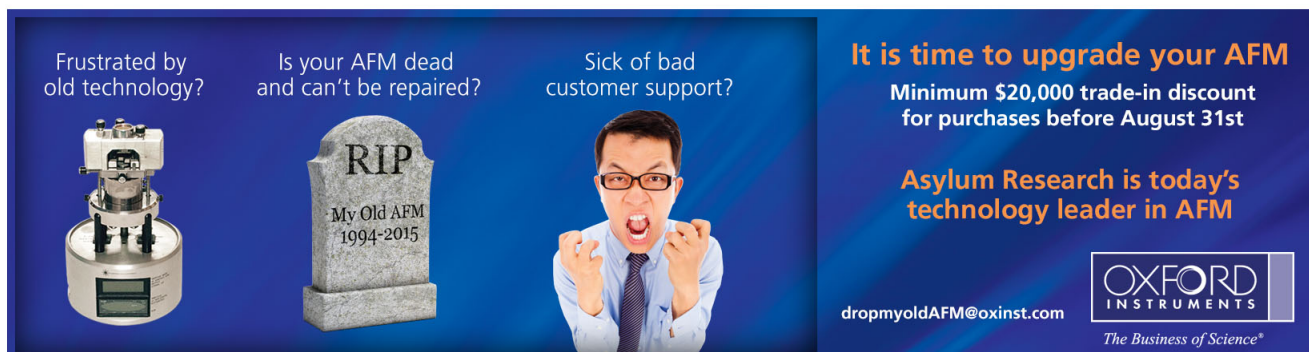Appl. Phys. Lett. **101**, 103901 (2012); 10.1063/1.4749810

Integrated photonic structures for light trapping in thin-film Si solar cells
Appl. Phys. Lett. **100**, 111110 (2012); 10.1063/1.3693613

Photonic crystal enhanced light-trapping in thin film solar cells
J. Appl. Phys. **103**, 093102 (2008); 10.1063/1.2908212

Light-trapping optimization in wet-etched silicon photonic crystal solar cells

Sergey Eyderman,[1,a)] Sajeev John,[1,2] M. Hafez,[2] S. S. Al-Ameer,[2] T. S. Al-Harby,[2] Y. Al-Hadeethi,[2] and D. M. Bouwes[3]

[1]*Department of Physics, University of Toronto, 60 St. George Street, Toronto, Ontario M5S 1A7, Canada*
[2]*Department of Physics, King Abdul-Aziz University, Jeddah, Saudi Arabia*
[3]*iX-factory GmbH, Konrad Adenauer–Allee 11, 44263 Dortmund, Germany*

We demonstrate, by numerical solution of Maxwell's equations, near-perfect solar light-trapping and absorption over the 300–1100 nm wavelength band in silicon photonic crystal (PhC) architectures, amenable to fabrication by wet-etching and requiring less than 10 μm (equivalent bulk thickness) of crystalline silicon. These PhC's consist of square lattices of inverted pyramids with sides comprised of various (111) silicon facets and pyramid center-to-center spacing in the range of 1.3–2.5 μm. For a wet-etched slab with overall height H = 10 μm and lattice constant a = 2.5 μm, we find a maximum achievable photo-current density (MAPD) of 42.5 mA/cm^2, falling not far from 43.5 mA/cm^2, corresponding to 100% solar absorption in the range of 300–1100 nm. We also demonstrate a MAPD of 37.8 mA/cm^2 for a thinner silicon PhC slab of overall height H = 5 μm and lattice constant a = 1.9 μm. When H is further reduced to 3 μm, the optimal lattice constant for inverted pyramids reduces to a = 1.3 μm and provides the MAPD of 35.5 mA/cm^2. These wet-etched structures require more than double the volume of silicon, in comparison to the overall mathematically optimum PhC structure (consisting of slanted conical pores), to achieve the same degree of solar absorption. It is suggested these 3–10 μm thick structures are valuable alternatives to currently utilized 300 μm-thick textured solar cells and are suitable for large-scale fabrication by wet-etching. © *2015 AIP Publishing LLC*. [http://dx.doi.org/10.1063/1.4926548]

I. INTRODUCTION

Multiple light scattering and wave interference effects provide a fundamental mechanism for light trapping. In a weakly absorbing medium, the resulting long dwell time for light enables significant absorption enhancement.[1] Photonic crystals (PhC's)[2,3] are special class of light-trapping materials in which this capability is often associated with suppression of the electromagnetic density of states.[4] A less widely studied form of photonic crystal light-trapping occurs when this density of states is enhanced rather than suppressed.[5] This alternative form of light trapping is useful for absorption of light from a broadband external source[6–8] and has been exploited for the design of thin-film (200 nm–1 μm) solar cells with high power conversion efficiencies.[9,10] Other applications of photonic crystals include optical interconnects,[11] imaging devices,[12] optical sensors,[13] and biosensors.[14] In this paper, we show that suitably structured, intermediate thickness ($\sim$10 μm) silicon photonic crystals can achieve solar light-trapping and absorption comparable to and possibly surpassing the best available[15] thick (300–450 μm) silicon solar cells.

Crystalline silicon wafers are currently the most widely used materials in the solar cell industry with up to 25% power conversion efficiency in a 300 μm thick wafer.[16] However, untextured crystalline silicon wafers have high solar reflectivity, around 40%, in the visible wavelength range and very weak absorption in the red to infrared spectral range. In order to improve the cell efficiency, anti-reflective surface texturing[17] is applied to crystalline silicon solar cells to reduce light reflection[18–20] at the wafer surface. If the lattice constant of surface texturing is large compared to the wavelengths of incident photons, the texture will induce light reflection between the surfaces of the texture, resulting in solar ray-trapping[21–26] and reduced light reflection.

On the other hand, if the period of the surface texture is comparable to or smaller than the wavelengths of incident photons, enhanced solar light-trapping can occur through multiple scattering and wave interference. In addition to reduced light reflection due to a graded refractive index near the surface, parallel-to-interface refraction (PIR)[5] and slow-light effects[6,19] lead to a strong light absorption in thin-film ($\sim$1 μm) silicon PhC solar cells even at near infrared wavelengths. This anomalous type of refraction is negative and usually out of the plane of incidence. Sunlight impinging on photonic crystal interface, couples to Bloch modes propagating nearly parallel to the interface. This leads to anomalously long optical path lengths and long dwell times before the light beam exits the thin film. This effect becomes especially pronounced in the wavelength region where intrinsic absorption of silicon is weak, manifesting itself as strong absorption peaks in the infrared region.

The PIR effect cannot be captured by ordinary ray tracing methods. This effect has purely wave nature and manifests itself as a parallel-to-interface energy flow as well as its circulation in certain areas.[7] Also despite the fact that the lattice constant is greater than a typical wavelength, our structure, described below (see Fig. 2), has areas (close to the tips

a)Author to whom correspondence should be addressed. Electronic mail: sergey.eyderman@utoronto.ca

of pyramids where they are narrowing), where the wavelength is comparable or even greater than the size of the structure. This further makes geometrical optics approach insufficient.

It was recently shown[7] that the mathematically optimum thin-film structure consists of a square lattice of slanted conical pores (Fig. 1).

This architecture simultaneously provides good antireflective and light trapping properties. With less than 1 μm equivalent bulk thickness of silicon, it is possible for this PhC to rival the solar absorption and power conversion efficiencies of conventional 300-μm-thick silicon wafers. This is possible with silicon exhibiting carrier diffusion lengths of less than 10 μm, provided that suitable surface passivation is applied. However, this thin-film architecture is not easily amenable to wet-etching fabrication methods and may require more advanced nano-imprinting and deposition techniques. In this paper, we describe an alternative PhC architecture, amenable to wet-etching, consisting of inverted pyramids rather than slanted cones, involving an intermediate thickness (3–10 μm) of silicon. While requiring more than double the volume of silicon compared to its slanted-cone counterpart, the inverted pyramid PhC's facilitate nearly perfect solar absorption using less than an order of magnitude volume of silicon than conventional silicon solar cells.

Texturing the top (100) surface of a silicon wafer is commonly achieved by wet-etching[27,28] using potassium hydroxide (KOH). In KOH, etching parallel to the silicon (111) crystal planes occurs 200 times faster than the etching parallel to (100) planes. When the fast etching (111) planes meet, etching is terminated. The etched depth is determined by the mask opening and the angle (of 54.7°) between the (111) and (100) planes. When the mask opening has a square shape, the four equivalent (111) planes meet, resulting in an inverted pyramid shape. A square lattice of such inverted pyramids provides a simplified approximant of the mathematically optimal slanted-pore PhC (see Fig. 2).

For comparison purposes, we begin by considering an infinitely thick silicon wafer perforated with a square array of inverted pyramids on the top, created by wet-etching. We
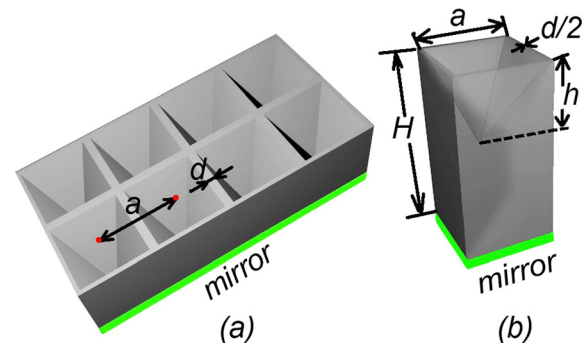
FIG. 2. (a) Top view of wet-etched PhC showing many periods, where "a" is a lattice constant and "d" is the separation between pyramid bases. (b) Inverted pyramid single unit cell, where "h" is the pyramid height and "H" is the total thickness of the structure.

retain a distance d = 100 nm between the sides of adjacent pyramid bases, as an aid in the wet-etching technique. We note, however, that the best solar absorption is achieved when the separation d = 0. The height of each pyramid is given by h = a_p/2*tan(α), where a_p = a−d is the base side length and α = 54.7° is the angle between the (111) and (100) planes. The solar absorption in this structure increases with lattice constant a (Fig. 3) but saturates to a MAPD of 38.3 mA/cm^2 for lattice constant a >2 μm (Fig. 4). For a = 1.5 μm, this structure provides an MAPD of 37.8 mA/cm^2, which is roughly 30% better than the MAPD for an unpatterned silicon wafer. We show below, that an improved MAPD of 40 mA/cm^2 is possible for H = 10 μm thick inverted pyramid PhC placed on a silver mirror with a lattice constant a = 2.5 μm (Fig. 6). This MAPD reduces to 37.8 mA/cm^2 when H = 5 μm at the lattice constant a = 2 μm and 35.5 mA/cm^2 when H = 3 μm at the lattice constant a = 1.3 μm (Fig. 6). These values are improved when the separation, d, between pyramid bases is reduced to zero and thin (~200 nm) surface passivation coating layer of SiO$_2$ is added on top of the silicon. In this case, a MAPD of 42.5 mA/cm^2 is realized for the H = 10 μm thick inverted pyramid PhC.
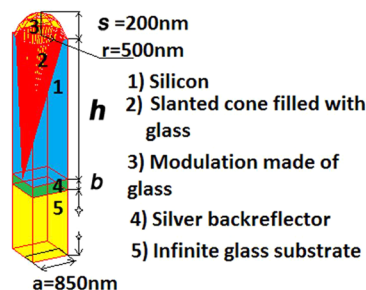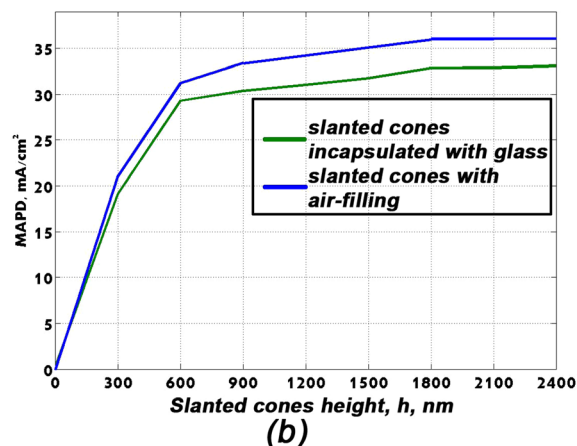
FIG. 1. (a) Mathematically optimum silicon PhC architecture for solar light-trapping and absorption consists of a periodic array of slanted conical pores with top radius r = 500 nm, lattice constant a = 850 nm and variable height h, placed on metallic back-reflector (for details see Ref. 7). (b) Depicted is the maximum achievable photo-current density of a PhC (with unit cell depicted in (a)) as a function of cone height h for the case of (i) air filling and in regions 2 and 3 (upper blue curve) and (ii) SiO$_2$ encapsulated filling regions 2 and 3 (lower green curve). The equivalent bulk thickness of silicon is given by dividing h by a factor of 1.6.
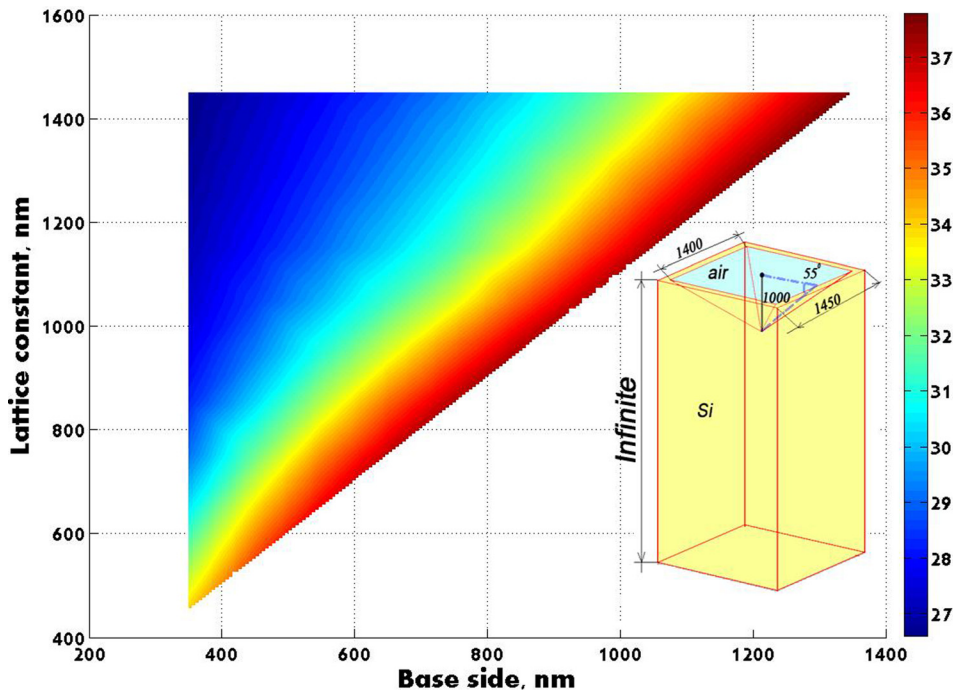
FIG. 3. Short circuit current (normal incidence of AM 1.5 sunlight) for inverted pyramids in bulk (H → ∞) silicon arranged in a square lattice and filled with air as function of the lattice constant, a, and the pyramid base side length $a_p = a–d$. The overall photonic crystal slab width is 300 μm. The angle between a lateral face and the base of pyramid is 54.7°. The optimal parameters lie along the lowest slanted line which corresponds to the minimal possible distance between the sides of pyramids of d = 100 nm. The MAPD shows a gradual growth along this line. The parameters corresponding to the highest MAPD achieved are shown in the inset. The color bar on the right indicates MAPD in units of mA/cm^2. The maximal photo-current density obtained is J = 37.8 mA/cm^2 (in the spectral range of 300–1100 nm) for a lattice constant a = 1400 nm. This continues to increase very slowly as is increased further (see Fig. 4).

There is significant difference in the optimal lattice constants for inverted pyramid and slanted conical pore structures. This difference is a result of the constraint implied by the wet-etching technique, namely, the dependence of pyramids height on the lattice constant. This constraint does not simultaneously allow the "ideal" antireflective and light-trapping properties. For ideal light-trapping of sunlight in the 800–1100 nm range, a smaller lattice constant is required. However, for inverted pyramids with a fixed etch angle, this would lead to a small depth and provide inadequate antireflection. The optimized inverted pyramid lattice constant is the best compromise between these two functions. There is no such constraint for our slanted conical pores, which would use a much different technique for fabrication. If, on the other hand, inverted pyramids of an arbitrary angle could be wet-etched, we expect that the optimal lattice constants would be similar for both structures.

In Sec. II, we describe our method of calculation. In Sec. III, we compare the optimized MAPD of a patterned 300 μm thick silicon wafer with intermediate thickness (3–10 μm) counterparts imposed on silver back-reflector. These, in turn, are benchmarked to the mathematically optimum slanted conical pore PhC's. In Sec. IV, we make concluding remarks.

II. METHOD OF SIMULATION

Numerical simulations are performed using the finite-difference time-domain (FDTD) method[29] with the help of
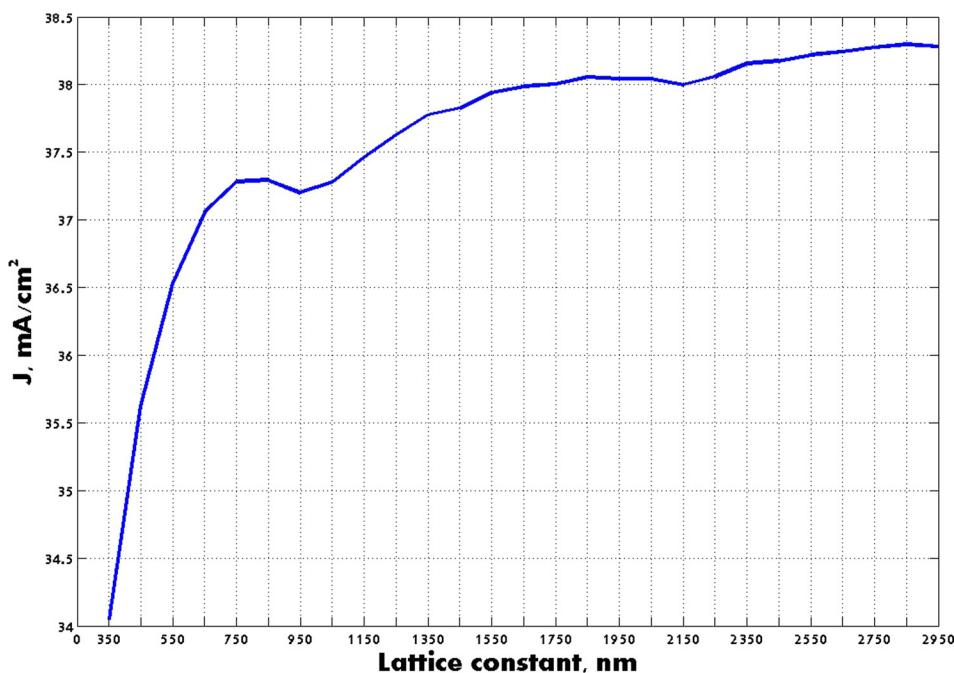

FIG. 4. Short circuit current (normal incidence of AM 1.5 sunlight) dependence on lattice constant for inverted pyramids on silicon, arranged in a square lattice and filled with air. The photonic crystal slab thickness is H = 300 μm (see Fig. 3). The distance between the sides of pyramids is 100 nm. Maximal short circuit current obtained is J = 38.3 mA/cm^2 for a = 2.8 μm in the spectral range of 300–1100 nm.
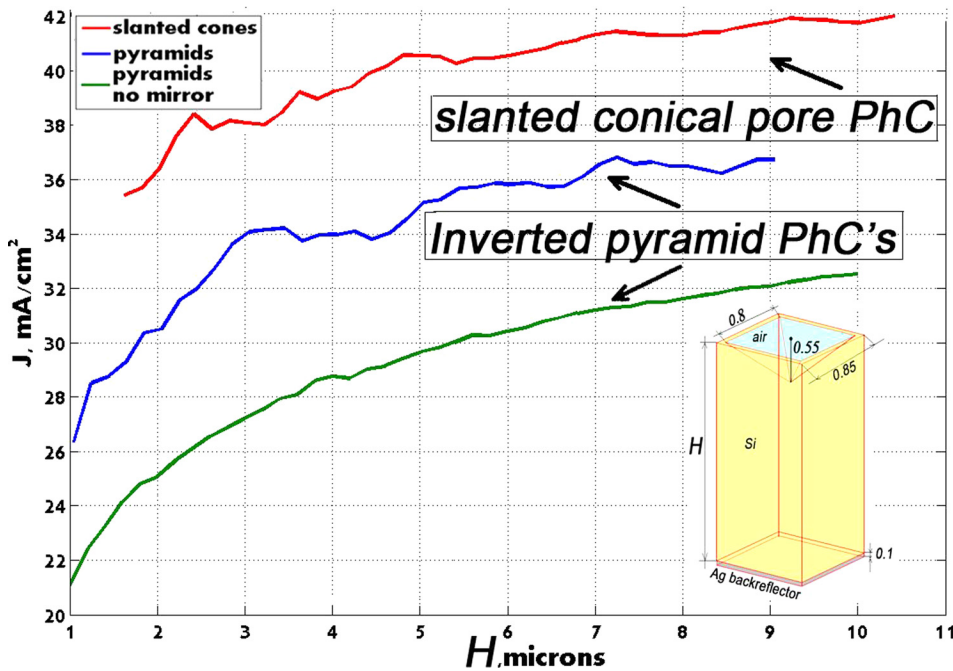
FIG. 5. Short circuit current dependence (normal incidence of AM 1.5 sunlight) on the height H of silicon wafer, with a = 850 nm and pyramid depth h = 550 nm, for three cases: (1) Inverted pyramids with no silver back-reflector (the structure is placed on an infinite glass substrate), (2) inverted pyramids placed on a silver back-reflector (see the inset), (3) slanted conical pores of depth 1.6 μm with the lattice constant a = 850 nm, base radius r = 500 nm and silver backreflector.

the Electromagnetic Template Library.[30] We use a standard scheme of the FDTD calculation in which propagation of a wave impulse through the structure is modeled. During the numerical experiment, the amplitudes of the reflected and transmitted waves are recorded, transformed to the frequency domain, and normalized by the incident spectrum. In this way, we obtain directly the transmission T(ω), reflection R(ω), and indirectly the absorption A(ω) = 1 − T(ω) − R(ω) coefficients for given light frequency ω, incident angle, and polarization. The absorption coefficient is also independently and directly evaluated using the formulae:

$$\alpha(\omega,\vec{r}) = \frac{\omega \cdot \mathrm{Im}(\varepsilon)|\vec{E}(\omega,\vec{r})|^2}{c \cdot \int \mathrm{Re}[\vec{E}_0 \times \vec{H}_0^*] \cdot \hat{n} \mathrm{d}x\mathrm{d}y}, \quad A(\omega) = \int \mathrm{d}^3\vec{r}\alpha(\omega,\vec{r}).$$

(1)

Here, ω is an angular frequency, E is the electric field amplitude calculated at each point of a computational grid located within silicon, ε is the frequency-dependent and complex dielectric permittivity of silicon, E_0 and H_0 are electric and magnetic vectors of the incident plane wave, $\hat{n}$ is a normal unit vector, and the superscript * indicates the complex conjugate. Both the direct and indirect methods for calculating the absorption give identical results. However, when the structure is imposed on a metallic substrate, the indirect method of absorption simulation also includes absorption in metal, which does not contribute to the MAPD. Therefore, this approach leads to a slight overestimate of the MAPD. In the present paper, we use an indirect method since it is less time and resource consuming. The overestimation of the MAPD does not exceed 0.6–0.8 mA/cm² depending on the geometry.

Experimental data on the silicon dielectric permittivity is taken from Ref. 31. The frequency dependence $\varepsilon(\omega)$ is assigned in the FDTD by considering a modified Lorentz model where dielectric polarization depends both on the

electric field and its first time derivative.[31] This model provides an accurate fit of the optical response of bulk crystalline silicon to sunlight over the wavelength range from 300 to 1100 nm, while conventional Debye, Drude, and Lorentz approximations fail. Fitting of the silicon dielectric function is found with the help of an open MATLAB program.[32]

The MAPD, in which all generated carriers are assumed to be collected, is calculated by integrating the simulated absorption with incident solar Air Mass 1.5 Global Spectrum[33] intensity I(λ) over the required wavelength range. Assuming that each absorbed photon is converted into a single electron-hole pair that is separated across a P-N junction and collected without recombination losses, we obtain the maximum achievable short circuit current for AM 1.5 solar spectrum[33] in the spectral window [λ_{min}, λ_{max}], all collimated into normal incidence

$$J = \int_{\lambda_{min}}^{\lambda_{max}} \frac{e\lambda}{hc} I(\lambda)A(\lambda)d\lambda.$$

(2)

Here, I(λ) is the incident AM 1.5 light intensity, A(λ) is the absorption coefficient obtained indirectly as A(ω) = 1 − T(ω) − R(ω), h is Planck's constant, e is the electronic charge, and c is the speed of light.

III. MAXIMAL SHORT CIRCUIT CURRENT CALCULATION

The short circuit current is an alternative measure of the total amount of AM 1.5 sunlight absorbed in a given structure. For 100% absorption of sunlight in the range of 300–1100 nm, the MAPD corresponds to 43.5 mA/cm². For reference purposes, we calculate the MAPD of a free-standing (with air above and air below) bulk silicon slab with the thickness of 300 μm. Calculating the absorption coefficient and using formula (2) in the spectral range of
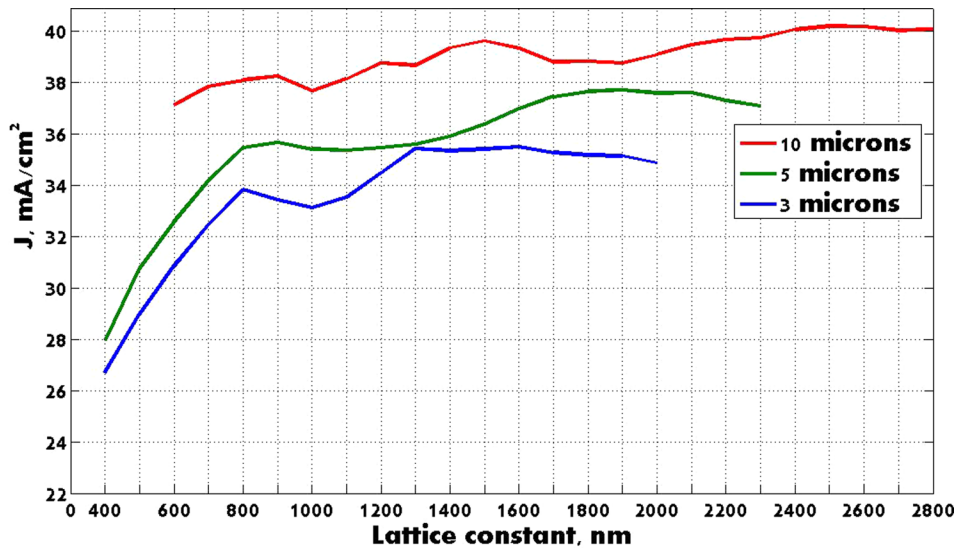
FIG. 6. MAPD (normal incidence of AM 1.5 sunlight) dependence on lattice constant for inverted pyramid PhC's in bulk silicon, arranged in a square lattice, and filled with air for three silicon heights. The structures are placed on silver back-reflectors. The distance between the sides of pyramids is 100 nm. Maximal short circuit current obtained is J = 35.5 mA/cm^2 for H = 3 μm and a = 1.3 μm, J = 37.8 mA/cm^2 for H = 5 μm and a = 1900 nm, and J = 40 mA/cm^2 for a = 2.5 μm and H = 10 μm in the spectral range of 300–1100 nm.

300–1100 nm, we obtain the MAPD of J = 26.1 mA/cm^2. In other words, only 60% of the AM 1.5 sunlight in the 300–1100 nm is absorbed. This flat-cell architecture lacks adequate light trapping and antireflective properties. We now consider the effect of optimized periodic arrays of inverted pyramids wet etched across the top surface for various thicknesses of silicon wafers (Fig. 2).

In Fig. 3, we present a map for MAPD optimization using an array of inverted pyramids in bulk (infinitely thick) silicon arranged in a square lattice. Sunlight is assumed collimated at normal incidence and the silicon pores are filled with air (n = 1). The structure shown in the inset of Fig. 3 provides a gradual increase of a MAPD with increasing pyramid base side length. The optimal parameters lie along the lowest slanted line which corresponds to the minimal possible distance of 100 nm between the sides of pyramids. We extend this region up to a = 3 μm (see Fig. 4).

Fig. 4 shows that the MAPD growth saturates after the lattice constant reaches 1.5 μm. When a = 1.5 μm and h = 1.1 μm, the MAPD is close to 38 mA/cm^2 in the 300–1100 nm wavelength range. This occurs for 100 nm distance between pyramids bases and is almost 30% better than the unpatterned silicon wafer reference case (with the MAPD of only 26.1 mA/cm^2). We find that the H = 300 μm thick silicon wafer and the semi-infinite wafer (H → ∞) give practically the same MAPD.

We examine the dependence of the MAPD on the silicon wafer thickness for intermediate values of H = 3–10 μm (Fig. 5). For this purpose, we fix the lattice constant a = 850 nm (the optimal value found for the slanted conical PhC), keeping the minimal possible distance between the sides of pyramids equal d = 100 nm. For a = 850 nm, the MAPD demonstrates a gradual increase with wafer thickness but begins to saturate when the overall thickness H ≈ 5 μm. We compare the MAPD dependence on the silicon wafer thickness, H, for three cases: (1) with no silver back-reflector (the PhC is placed on an infinite glass substrate), (2) with silver back-reflector (see Fig. 2b), and (3) mathematically optimized slanted conical pore PhC with the lattice constant

a = 850 nm and base radius r = 500 nm,[7] placed on a silver back-reflector (Fig. 1).

For the specific choice of a = 850 nm, the slanted conical pore PhC (red curve) exhibits better performance than wet-etched structure of the same overall height H by about 3–5 mA/cm^2. We find a MAPD J = 35.5 mA/cm^2 in the spectral range of 300–1100 nm for H = h = 1.6 μm wafer thickness, which corresponds just 1 μm effective bulk thickness of silicon.[7] As the thickness of slanted pore PhC is increased to H = 10 μm (h remains equal 1.6 μm), the MAPD reaches almost J = 42 mA/cm^2, only slightly below the perfect solar absorption value of 43.5 mA/cm^2.

For the inverted pyramid PhC with lattice constant a = 850 nm (Fig. 5 blue curve), when the overall height H = 1.6 μm (1.43 μm equivalent bulk thickness) the MAPD is about J = 29 mA/cm^2. As the wafer thickness H increases, the MAPD reaches almost J = 37 mA/cm^2 at H = 9 μm. This is just slightly below the MAPD for a 300 μm thick wafer with the same lattice periodicity. For calibration purposes and to delineate the role of the silver back-reflector, we also calculate the dependence of the MAPD on H for an inverted pyramid PhC's (with a = 850 nm) sitting on a semi-infinite glass substrate (green curve). In this case, the MAPD reaches only J = 32.5 mA/cm^2 for H = 10 μm.

For inverted pyramid PhC's, the optimal lattice constant is considerably larger than for the slanted conical pore PhC. Substantial improvements in the MAPD for H = 3, 5 and 10 μm thick inverted pyramid PC's are found when "a" is increased to 1.3 μm, 1.9 μm, and 2.5 μm, respectively (see Fig. 6).

For an inverted pyramid PhC with H = 3 μm (blue curve), the MAPD reaches its maximum of 35.5 mA/cm^2 for a = 1.3 μm. In the case of H = 5 μm, this maximum shifts to a = 1.9 μm and the MAPD J = 37.8 mA/cm^2. This latter value coincides with the best MAPD achieved for a 300 μm thick wafer patterned with inverse pyramids (see Fig. 4). Finally, for H = 10 μm, the optimum lattice constant is a = 2.5 μm, for which the MAPD of J = 40 mA/cm^2 is found.

We also investigate the influence of an anti-reflection coating (ARC) on the MAPD. A thin layer of SiO$_2$ on the surface can provide additional antireflective properties and at
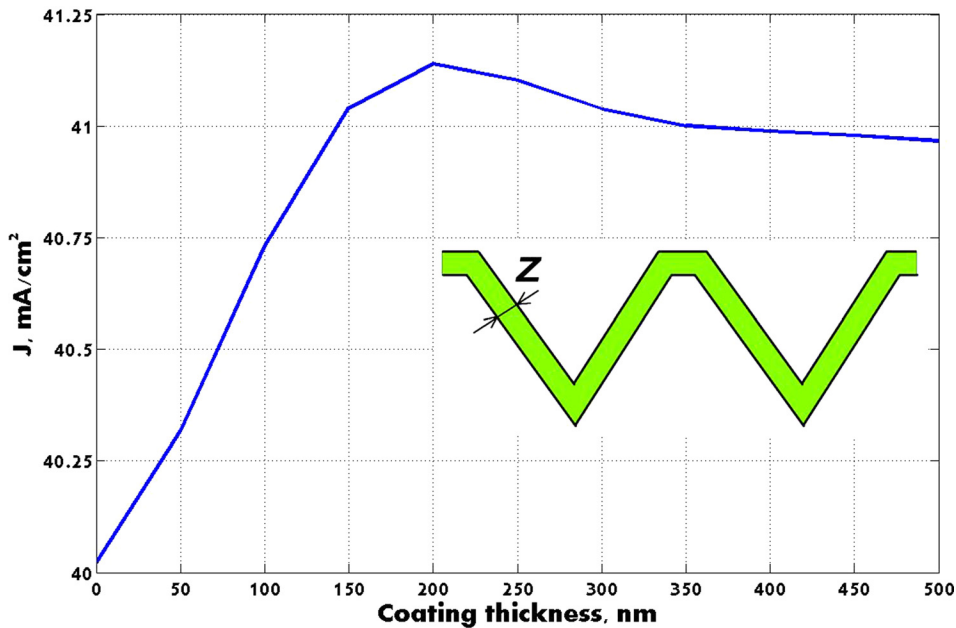
FIG. 7. The MAPD dependence on the conformal coating thickness z for inverted pyramids in silicon placed on a silver back-reflector. The coating, consisting of glass with the refractive index $n = 1.45$, is schematically depicted in the inset. The overall height of silicon is $H = 10\,\mu m$ and the lattice constant $a = 2.5\,\mu m$. The distance between the sides of silicon pyramids is 100 nm. Maximal short circuit current obtained is $J = 41.1\,mA/cm^2$ for $z = 200\,nm$.

the same time passivate the silicon surface from unwanted carrier recombination. In our simulations, we consider a conformal, non-absorbing coating with a refractive index $n = 1.45$ (see the inset in Fig. 7).

We consider the best case achieved in Fig. 6. Namely, the overall height of the structure is $H = 10\,\mu m$ and the lattice constant $a = 2.5\,\mu m$. For these parameters, the MAPD of $J = 40\,mA/cm^2$ is found. It is seen that the MAPD increases with glass coating thickness, z, and reaches its maximum of $41.1\,mA/cm^2$ for $z = 200\,nm$. By including this antireflective passivation layer, we gain an additive contribution of $1.1\,mA/cm^2$ to solar cell performance. Furthermore, if the spacing between the sides of pyramids of 100 nm is removed ($d = 0$), we attain a MAPD of $42.5\,mA/cm^2$.

IV. CONCLUSION

In conclusion, we have identified a set of intermediate thickness $(3–10\,\mu m)$ silicon photonic crystals that enable strong light-trapping and solar absorption in the 300–1100 nm wavelength range. These structures require one to two orders of magnitude less silicon than conventional silicon solar cells used today, but provide a maximum achievable photocurrent density comparable to or even better than their much thicker counterparts. Our intermediate thickness photonic crystals are amenable to large-scale fabrication by wet-etching, making them an attractive alternative to previously identified (mathematically optimum) structures consisting of a lattice of slanted conical pores. Unlike, the slanted conical pores that require a curved surface profile, our intermediate thickness, inverted pyramid structures involve flat (111) and (100) surfaces of silicon. Our best 10-μm thick inverted pyramid PhC offers a MAPD of $40\,mA/cm^2$, compared to the corresponding slanted conical pore PhC with the MAPD of $42\,mA/cm^2$ and compared to the perfect solar absorption limit of $43.5\,mA/cm^2$. With a suitable surface passivation layer, an additive $1.1\,mA/cm^2$ is obtained for the inverted pyramid PhC. When the spacing

between the sides of the inverted pyramids is removed ($d = 0$ in Fig. 2), we gain an additional $1.4\,mA/cm^2$ to reach our best MAPD of $42.5\,mA/cm^2$ for a 10-μm-height inverted-pyramid silicon photonic crystal. Even higher MAPD is expected for slanted-conical-pore photonic crystals of comparable thickness. These results are obtained by studying a relatively unexplored regime of thickness where novel wave effects and light-trapping phenomena, remarkably, enable better solar absorption than in a $300\,\mu m$ thick silicon solar cell. Given, the shorter carrier diffusion length required in a 10-μm-thick silicon PhC solar cell, it is anticipated that this architecture may provide higher power conversion efficiency than currently employed thick (100–300 μm) silicon solar cells. A recent study of black silicon[34] shows that surface recombination velocities can be reduced to $\sim 10\,cm/s$ if the silicon surface is treated by conformal atomic layer deposition of Al_2O_3. These results suggest that using a factor of 30 less active material, intermediate thickness silicon photonic crystals can approach and possibly surpass the current world record power conversion efficiency (of about 25%) for silicon solar cells.

ACKNOWLEDGMENTS

[1]S. John, "Electromagnetic absorption in a disordered medium near a photon mobility edge," Phys. Rev. Lett. **53**, 2169 (1984).
[2]S. John, "Strong localization of photons in certain disordered dielectric superlattices," Phys. Rev. Lett. **58**, 2486 (1987).
[3]E. Yablonovitch, "Inhibited spontaneous emission in solid-state physics and electronics," Phys. Rev. Lett. **58**, 2059 (1987).
[4]S. John and R. Rangarajan, "Optimal structures for classical wave localization: An alternative to the Ioffe-Regel criterion," Phys. Rev. B **38**, 10101 (1988).

[5]A. Chutinan and S. John, "Light trapping and absorption optimization in certain thin-film photonic crystal architectures," Phys. Rev. A **78**, 023825 (2008).

[6]G. Demesy and S. John, "Solar energy trapping with modulated silicon nanowire photonic crystals," J. Appl. Phys. **112**, 074326 (2012).

[7]S. Eyderman, S. John, and A. Deinega, "Solar light trapping in slanted conical-pore photonic crystals: Beyond statistical ray trapping," J. Appl. Phys. **113**, 154315 (2013).

[8]S. Eyderman, A. Deinega, and S. John, "Near perfect solar absorption in ultra-thin-film GaAs photonic crystals," J. Mater. Chem. A **2**, 761–769 (2014).

[9]A. Deinega and S. John, "Solar power conversion efficiency in modulated silicon nanowire photonic crystals," J. Appl. Phys. **112**, 074327 (2012).

[10]A. Deinega, S. Eyderman, and S. John, "Coupled optical and electrical modeling of solar cell based on conical pore silicon photonic crystals," J. Appl. Phys. **113**, 224501 (2013).

[11]X. Zhang and A. Hosseini, "Polymer-based hybrid integrated photonic devices for silicon on-chip modulation and board-level optical interconnects," IEEE J. Sel. Top. Quantum Electron. **19**(6), 3401115 (2013).

[12]J. Yu *et al.*, "Characterization and application of chirped photonic crystal fiber in multiphoton imaging," Opt. Express **22**(9), 10366–10379 (2014).

[13]X. Zhang *et al.*, "Integrated photonic electromagnetic field sensor based on broadband bowtie antenna coupled silicon organic hybrid modulator," IEEE J. Lightwave Technol. **32**(20), 3774–3784 (2014).

[14]A. Al-Rashid and S. John, "Optical bio-sensing of multiple disease markers in a photonic-band-gap lab-on-a-chip: A conceptual paradigm," Phys. Rev. Appl. **3**, 034001 (2015).

[15]T. Saga, "Advances in crystalline silicon solar cell technology for industrial mass production," NPG Asia Mater. **2**(3), 96 (2010).

[16]M. A. Green, "The path to 25% silicon solar cell efficiency: History of silicon cell evolution," Prog. Photovoltaics: Res. Appl. **17**, 183–189 (2009).

[17]P. Campbell and M. Green, "Light trapping properties of pyramidally textured surfaces," J. Appl. Phys. **62**, 243–249 (1987).

[18]F.-J. Haug *et al.*, "Resonances and absorption enhancement in thin film silicon solar cells with periodic interface texture," J. Appl. Phys. **109**, 084516 (2011).

[19]A. Deinega, I. Valuev, B. Potapkin, and Yu. Lozovik, "Minimizing light reflection from dielectric textured surfaces," JOSA A **28**, 770–777 (2011).

[20]P. Bermel, C. Luo, L. Zeng, L. C. Kimerling, and J. D. Joannopoulos, "Improving thin-film crystalline silicon solar cell efficiencies with photonic crystals," Opt. Express **15**(25), 16986 (2007).

[21]J. Gjessing *et al.*, "Comparison of periodic light-trapping structures in thin crystalline silicon solar cells," J. Appl. Phys. **110**, 033104 (2011).

[22]E. Garnett and P. Yang, "Light trapping in silicon nanowire solar cells," Nano Lett. **10**(3), 1082–1087 (2010).

[23]P. Kuang, A. Deinega, M.-L. Hsieh, S. John, and S.-Y. Lin, "Light trapping and near-unity solar absorption in a three-dimensional photonic-crystal," Opt. Lett. **38**(20), 4200 (2013).

[24]X. Sheng, L. Z. Broderick, and L. C. Kimerling, "Photonic crystal structures for light trapping in thin-film Si solar cells: Modeling, process and optimizations," Opt. Commun. **314**, 41–47 (2014).

[25]X. H. Li *et al.*, "Light trapping in thin-film solar cells via scattering by nanostructured antireflection coatings," J. Appl. Phys. **114**, 044310 (2013).

[26]X. Li, *et al.*, "Subwavelength nanostructures integrated with polymer-packaged III–V solar cells for omnidirectional, broad-spectrum improvement of photovoltaic performance," Prog. Photovoltaics: Res. Appl. (published online).

[27]H.-H. Lin and W.-H. Chen, "Improvement of polycrystalline silicon wafer solar cell efficiency by forming nanoscale pyramids on wafer surface using a self-mask etching technique," J. Vac. Sci. Technol., B **31**(3), 031401 (2013).

[28]T. Deng, J. Chen, C. N. Wu, and Z. W. Liu, "Fabrication of inverted-pyramid silicon nanopore arrays with three-step wet etching," ECS J. Solid State Sci. Technol. **2**(11), 419–422 (2013).

[29]A. Taflove and S. C. Hagness, *Computational Electrodynamics: The Finite-Difference Time-Domain Method*, 3rd ed. (Artech House Publishers, 2005).

[30]See http://fdtd.kintechlab.com for Electromagnetic Template Library (EMTL), Kintech Lab Ltd.

[31]A. Deinega and S. John, "Effective optical response of silicon to sunlight in the finite-difference time-domain method," Opt. Lett. **37**, 112 (2012).

[32]See http://fdtd.kintechlab.com/en/fitting for Fitting of dielectric function.

[33]See http://rredc.nrel.gov/solar/spectra/am1.5/ for Reference Solar Spectral Irradiance: Air Mass 1.5.

[34]H. Savin *et al.*, "Black silicon solar cells with interdigitated back-contacts achieve 22.1% efficiency," Nat. Nanotechnol. **10**, 624–628 (2015).